Design of nalidixic acid-vanadium complex loaded into chitosan hybrid nanoparticles as smart strategy to inhibit bacterial growth and quorum sensing

Bárbara Bueloni[1], Daniele Sanna[2], Eugenio Garribba[3], Guillermo R. Castro[1], Ignacio E. León[4*], Germán A. Islan[1*]

[1]Laboratorio de Nanobiomateriales, CINDEFI, Departamento de Química, Facultad de Ciencias Exactas, Universidad Nacional de La Plata (UNLP) -CONICET (CCT La Plata), Calle 47 y 115, (B1900AJI), La Plata, Buenos Aires, Argentina.

[2]Istituto di Chimica Biomolecolare, Consiglio Nazionale delle Ricerche, trav. la Crucca 3, 07100 Sassari, Italy

[3]Dipartimento di Chimica e Farmacia, Unversità di Sassari, Via Vienna 2, 07100 Sassari, Italy

[4]Centro de Química Inorgánica (CEQUINOR, UNLP-CONICET, CCT La Plata). Universidad Nacional de La Plata, Bv 120 1465, La Plata, Argentina.

*** Correspondence:**

Dr. German A. Islan
Tel./fax: +54 221 4833794
E-mail: germanislan@biol.unlp.edu.ar

Dr. Ignacio E. León
E-mail: ileon@biol.unlp.edu.ar

Abstract

The discovery of new alternatives for the treatment of infectious diseases has become the focus of burgeoning global interest. The complexation of the wide-spectrum antibiotic nalidixic acid (NA) with oxidovanadium(IV) ion and its incorporation into hybrid nanoparticulate systems were explored. The V-NA complex proved to be a stronger antimicrobial agent against *E. coli, B. cereus, S. aureus* and *P. aeruginosa* than NA, based on inhibition experiments. Myristyl myristate nanostructured lipid carriers (NLCs) and polymeric nanoparticles of Eudragit NE30D (EuNPs) were hybridized with chitosan (chi) to increase their stability and mucoadhesivity. They showed V-NA encapsulation of 97.8±0.5% and 96.1±0.1% respectively. TEM and DLS characterization ascertained the presence of spherical positive charged NPs ranging from 170 -330 nm. Controlled release of V-NA from NPs was observed with 30-40% release in 3 days. A considerable potentiation of V-NA antimicrobial activity from 5-10 times was elucidated against *P. aeruginosa* with MIC values of 59.3 and 129.9 μM for NLC/chi and EuNPs/chi respectively, in comparison with 625 μM of the free complex. Hybrid NPs were able to interfere with the *quorum sensing* of the reporter *Chromobacterium violaceum*. Cytotoxicity on mouse fibroblast L929 cells was evaluated in the range of 29.7-519 μM by MTT assay showing that, NLC/chi particles supported cell growth in the range of at 29.7- 60 μM whilst Eu/chi do not exert cytotoxicity between 29.7-120 μM. These results suggest that nanoparticles are-suitable systems for drug delivery applications.

Keywords: nanostructured lipid carriers, eudragit nanoparticles, chitosan, quorum sensing, vanadium, nalidixic acid

1. Introduction

Extensive use of current antibiotics exerts a selective pressure on occasional mutational events that confers microorganism multidrug resistance (MDR), giving rise to the one of the most relevant health issues nowadays [1]. In this context, stamped by the imperative need of discovering new antibiotics against biofilm-forming and multidrug-resistant bacteria, metal complexes have grown in popularity as potential antimicrobial agents [2]. The undeniable appealing of coordination compounds derives, at least in part, from the possibility of combining different metals and ligands with intrinsic pharmacological properties, thus dispensing with the discovery or invention of novel antibiotics. The increase in antimicrobial activity of biocides through their complexation with metals is strongly connected to the architecture of the resulting complex, and therefore to their physicochemical properties [3].

Vanadium is an ultra-trace metal with several biological effects, including insulin-mimetic [4,5], osteogenic [6], antiparasitic [7] and antitumoral [8–10]. The formation of vanadium complexes is thought to be an effective approach for increasing its solubility, as well as for improving its stability and absorption, thus modifying its biological and/or pharmacological effects [11]. Based on these considerations, vanadium compounds have recently emerged as non-platinum antitumor agents showing, among others, promising anticancer and antibacterial activity [11,12]. Nevertheless, many scientific reports described certain levels of toxicity of vanadium complexes on cell in culture and animals suggesting the use of new technologies in order to minimize the side effects [13–15].

The last decades have also witnessed an increasing impact of nanotechnology on medicine, emerging a great variety of nanoparticle-based drug delivery systems such as liposomes, nanoemulsions, micelles, solid lipid nanoparticles (SLNs), nanostructured lipid carriers (NLCs) and polymeric nanoparticles [16–19]. Nanoparticles (NPs) were proposed as suitable candidates for the delivery of antimicrobial agents [20,21]. The association of a drug with specific nanoparticles strongly influences the biodistribution profile and the reaching to target organs such as bone marrow, spleen, liver, or

lungs. Different factors like hydrophobicity of the material and composition may determine the in vivo fate of NPs [22]. Considering the low solubility of the V-NA complex two alternatives were explored as a strategy to increase its bioavailability: NLCs and polymeric NPs. The NLCs are considered as a second generation of SLNs, incorporating a small proportion of a liquid lipid that nano-structures the architecture of the lipid matrix, and have been associated to a greater drug loading capacity and to the prevention of drug expulsion during storage [23]. They provide increased drug loading, long term storage stability, cytocompatibility and extend the half-life. NLCs demonstrate to be safe and effective for parenteral, oral, inhalational, ocular, and dermal delivery. Some limitation of these systems could be associated with a burst release of the drug by erosion mechanism or accumulation of the lipids in the liver and spleen that cause some physiological pathologies [24,25]. As an alternative, polymeric systems have been reported as suitable carriers for different drugs. They can improve the delivery of proteins, antigens and drugs by different administration routes. Also, polymeric nanoparticles usually show low cytotoxicity and good cytocompatibility. However, the chemistry of the synthesized polymer materials could influence the absorption and the biodegradability of the developed carriers [26].

Moreover, NP can be tailored to obtain different biophysical properties by the selection of matrix composition, preparation method and surface modification with different molecules [27]. Myristyl myristate is a natural lipid with a low melting point (40 ºC) that has been successfully employed to produce NLCs which were particularly useful for the encapsulation of thermolabile compounds [21]. Eudragit NE 30 D is an aqueous dispersion of a neutral copolymer based on ethyl acrylate and methyl methacrylate. As matrix for polymeric nanoparticles, Eudragit NE 30 D

suitability was evaluated since previous studies have reported its use for potential development of drug delivery related applications [28]. Chitosan (Chi) is a biopolymer with several positively charged amine groups, hence its interaction with negatively charged bacterial cell wall. Recently, the adsorption of Chi on nanoparticles surface results on an increased mucoadhesion, enhanced stability that could improve the therapeutic effects of the drug carriers [20].

Recently, studies from our group examined the binding capability of nalidixic acid (NA) and other quinolone ligands towards oxidovanadium(IV) ion, assuming a possible synergistic effect of the metal and quinolones on the antimicrobial action of the complexes [29]. The complex vanadium-nalidixic acid, $[VO(NA)_2(H_2O)]\cdot 2H_2O$, here abbreviated with V-NA, was also synthesized and fully characterized. Moreover, the composition and structure of the species existing in aqueous solution at physiological pH was determined with a combination of spectroscopic and computational methods as well as their interaction with human blood serum proteins like albumin and transferrin [29]. The development of a NA complex aims to increase the potency of the antibiotic, since the growth of the number of microorganisms resistant to NA has risen considerably in the last years. The development of a new generation of quinolones with higher antimicrobial activity against different pathogens practically displaced NA from the conventional therapeutic uses [30]. Keeping in mind the lack of novel antibiotics in the global market during the last decades and the emergence of MDR bacteria, repositioning old drugs could be a feasible alternative from technological and sanitary points of view. Another aspect to considered is that NA is poorly soluble in water (100 mg/L at 23 °C). It can be dissolved in ethanol (0.9 mg/ml) or in chloroform, but that solvents result toxic for cells. On the other side, the different forms of vanadium (oxidovanadium (IV) and oxidovanadium (III)) are also insoluble in water [31]. The development of novel complexes often results in an increased solubility of the compound in comparison with the free components. However, vehiculization into NPs became necessary to finally obtain stable formulations suitable for biological applications.

The present work proposes the encapsulation of the complex V-NA as an alternative avenue for overcoming bacterial resistance to NA. The biocidal activity of the V-NA was examined, as well as

the antibacterial capacity of the encapsulated forms against Gram-positive and Gram-negative pathogens, including the study of its effect on swarming motility and quorum sensing respectively. Chi-coated Eudragit nanoparticles and myristyl myristate NLCs were proposed as smart biocarriers for the encapsulation and controlled release of the drug. The selective toxicity of V-NA complex was evaluated in mouse fibroblast L929 cell line model.

2. Materials and methods

2.1. Materials

Myristyl myristate (Crodamol™ MM) and the oil (Crodamol™ GTCC-LQ) were kindly donated by Croda (Argentina), the aqueous dispersion of Eudragit® NE30D was donated by Etilfarma (Argentina). Pluronic® F68, medium molecular weight Chi (190-310 kDa., 75-85% deacetylated) and 3-(4,5-Dimethyl-2-thiazolyl)-2,5-diphenyl-2H-tetrazolium bromide (MTT) were obtained from Sigma-Aldrich (Buenos Aires, Argentina). The Live/Dead BacLight® was purchased from Invitrogen™ (ThermoFisher, USA). Dulbecco's Modified Eagle'sMedium (DMEM) and TryplE™ were provided by Gibco (Invitrogen Corporation, USA). Fetal bovine serum (FBS) was purchased from Internegocios™ (Argentina). *Escherichia coli* ATCC 25922*, Pseudomonas aeruginosa* ATCC 27853*, Staphylococcus aureus* ATCC 25923*, Bacillus cereus* ATCC 10876 and *Chromobacterium violaceum* ATCC were donated by *Cátedra de Microbiología* (*Facultad de Ciencias Exactas, UNLP, Argentina*). L929 cells were purchased on ATCC.

Other reagents were of analytical grade from Merck (Darmstadt, Germany) or similar brands. Ultrapure water (Milli-Q grade, 0.22 μm filtered) was used in the preparation of solutions.

2.2. Complex synthesis

The complex $[VO(NA)_2(H_2O)]\cdot 2H_2O$ was synthesized as reported in the literature [29], following the procedure established by Psomas *et al.* [32]. Briefly, 15.0 mL of a methanolic solution of nalidixic acid (400 μM) deprotonated with KOH and 10 mL of a methanolic solution of $VOSO_4\cdot 3H_2O$ (200 μM) were mixed. After being refluxed for 2 h, the reaction mixture was filtered and left for slow evaporation at room temperature. The green microcrystalline product deposited after

a few days was filtrated, washed with methanol and dried. Later, the product was identified by elemental analysis, and FT-IR and EPR spectroscopy. Anal. calc. (%) for $[VO(NA)_2(H_2O)]\cdot 2H_2O$, $C_{24}H_{28}N_4O_{10}V$ (583.44): C, 49.41, H, 4.84, N, 9.60. Exptl. (%): C, 49.85; H, 4.51; N, 9.51. FT-IR analysis (ν_{max}/cm^{-1}): ν(O–H), 3410(m); ν_{as}(COO), 1636(ν_s); ν(C=O)$_{ket}$, 1605(vs); ν_s(COO), 1384(s); ν(V=O), 972(s). Spin-Hamiltonian EPR parameters: g_z, 1.945; A_z, 168.7×10^{-4} cm^{-1}.

2.3.Antimicrobial assays

2.3.1.*Minimum inhibitory concentration (MIC) and half maximal inhibitory concentration (IC_{50})*

Antimicrobial capacity of the antibiotic and the free complex was compared by the determination of MIC and IC_{50} against clinically relevant strains such as *Escherichia coli* ATCC 25922, *Pseudomonas aeruginosa* ATCC 27853, *Staphylococcus aureus* ATCC 25923 and *Bacillus cereus* ATCC10876. Briefly, serial dilutions in 100 µL of Mueller-Hinton (MH) broth of the stock solutions (20 µM, DMSO) of the formulations were made in a 96-well microtiter plate. Microwells were immediately inoculated with 100 µL inoculum of each bacteria previously grown for 24 h, adjusted to 0.5 McFarland and 1/100 diluted in MH broth. After overnight incubation at 37 ºC, MIC values were recorded visually as the lowest concentrations of the compounds that generate a complete inhibition of bacterial growth. For IC_{50} calculation, the absorbance (λ = 600 nm) was measured in a microplate reader (TECAN Infinite 200 PRO, Germany). The obtained data was converted into growth inhibition (%) and graphed against drug concentration and the IC_{50} was estimated by interpolation.

The same protocol was followed to determine antibacterial activity of the nanoencapsulated V-NA complex against the biofilm-forming strains *P. aeruginosa* and *S. aureus*. Particularly, growth inhibition of *P. aeruginosa* in presence of empty nanoparticles was included as control. Since the turbidity of the dispersion precluded visual determination of MICs, plates were revealed by the resazurin assay after incubation [33]. A solution of 0.015% resazurin (30 µL) was dropped into each well, prior to a period of 2 hours of incubation in darkness at room temperature. MICs were spotted as the lowest concentration of blue non-fluorescent resazurin was not reduced to the pink fluorescent

resorufin, since the reduction of the dye indicates metabolic activity. Each concentration was tested in triplicate, including growth and sterility controls for the medium.

2.3.2.*Antibiogram*

Agar disk-Diffusion method have been used to evaluate the growth inhibition effectiveness of the V-NA complex and its ligand according to International Clinical Standards (CLSI/NCCLS).The assay was performed with little modification of the standard procedure by the replacement of disk with sterile glass cylinders and performed in duplicate against as *E. coli* ATCC 25922, *P. aeruginosa* ATCC 27853, *S. aureus* ATCC 25923 and *B. cereus* ATCC 10876. Two cylinders were placed on MH agar plates, previously seeded with an adjusted suspension (0.5 McFarland scale) of each bacterium. Samples (50 µL) of 10 mM NA and 100 µM V-NA were dropped into the cylinders. Inhibition diameters zones (ZOI) were measured at 37 ºC after 24 h incubation

2.3.3.*Minimum bactericide concentration (MBC)*

MBC is defined as the lowest concentration of an agent that produces total bacterial cell death. Adopting the definition of bacterial death as irreversible loss of growth capacity, the medium from the 96-wells plaque used for MIC determination was subcultured onto a plate with sterile MH agar for *S. aureus, P. aeruginosa* and *B.cereus* and with Mc Conkey agar for *E. coli*. For each strain, the four wells following the last turbid well included as positive control where no visible growth was observed, were plated on identified position of the agar, and the lowest concentration at which colony formation remained absent incubated at 37 ºC after 24 h was taken as the MBC. The experiments were performed in triplicates.

2.3.4.*Staining cells with Live/Dead BacLight® kit*

Cell membrane integrity was used as criteria for complementing antibacterial potential comparison of NA and V-NA using the LIVE/DEAD BacLight® commercial kit, which combines a green-fluorescent SYTO9® and red-fluorescent propidium iodide stains [34]. Briefly, a volume of 20 µL of melted soft nutritive agar inoculated with each one of the four strains growing at late exponential phase was deposited on the surface of sterile glass slides for its incubation at 37 ºC for 24 h. The

ensuing cell monolayers were covered with 20 µL of 100 µM NA and V-NA, sodium hypochlorite (dead control, data not shown) or physiological solution (live control). Samples were carefully washed with deionized water after 1 h treatment, which were subsequently stained with a mixture of both dyes (0.75 µL of each one in 0.5 mL of sterile deionized water) and held in darkness for 20 min. Finally, all samples were washed using deionized water and analyzed in a epifluorescence microscope (Leica DM 2500, Germany). Viable bacteria emitted green fluorescence observed with U-MWG2 filters (λ_{ex} = 510-550 nm and λ_{em} = 590 nm), and damaged bacteria were seen red with U-MWB2 filters (λ_{ex} = 460 nm and λ_{em} = 490-520 nm).

2.3.5.*TEM observations*

Aliquots of 1.0 mL of inoculum at exponential bacterial growth were centrifuged at 5,000 × *g* for 5 min. The pellets containing the cells were washed with physiological solution and resuspended in 1.0 mL of physiological solution supplemented with V-NA complex (in a concentration that doubled the corresponding CIM value). Untreated samples were included as positive controls. The suspensions were ten-fold diluted in ultrapure water for TEM observation after 24 h as previously described.

2.3.6.*Swarming motility assay*

Considering the close relation between swarming motility and biofilm formation (O'May et al., 2011), and looking for the characterization of V-NA antimicrobial properties, the effect of the complex on *P. aeruginosa* and *S. aureus* was evaluated. Inoculum of 20 µL of each bacteria were dropped in the center of 0.4% soft nutritive agar plates containing 50, 100 and 200 µM of the V-NA complex. The V-NA complex was dissolved in DMSO to reach a final concentration of 10 mM, and subsequently added to the melted agar in a test tube to assure the homogenization of the solution, prior to pouring it in the plates. Control plates were prepared adding equivalent amounts of DMSO. All plates were incubated at 37 ºC and photographically recorded after 1, 2 and 7 days.

2.4 Hybrid NLCs preparation

Chi-coated NLCs containing the complex V-NA were synthesized by homogenization by ultrasonication [20]. Concisely, 10.0 mg of V-NA was dissolved in a mass of 400 mg of MM (2.0%, w/v) previously melted and 50 µl of oil, in water bath at 60 ºC. Then, 10 ml of a hot aqueous solution of Pluronic F68 (3.0%, w/v) and chitosan (0.2%, w/v) was subsequently added. The resulting suspension was immediately subjected to sonication in order to prevent a temperature drop that could result in the solidification of the lipid. The sonication was performed in an ultrasonic processor at 80% amplitude equipped with a 6 mm titanium tip for 15 minutes (130 Watts, Cole-Parmer, USA). Later, the dispersion was cooled down and stored at 5 ºC for further uses.

The stock solution of 2.0 % (w/v) chitosan was previously prepared in 0.2 M of acetic acid/sodium acetate buffer at pH=5.0 and 40 ºC under magnetic stirring. After complete dissolution, the solution was ten times diluted in the pluronic phase.

2.5. Hybrid polymeric nanoparticles preparation

Chi-coated polymeric nanoparticles were prepared following similar protocol than that for NLCs preparation. Briefly, 10.0 mg of V-NA were dissolved in 1.33 mL of 30% (w/v) Eudragit NE 30D at 60 ºC. A volume of 10 ml of a thermostarized solution of Pluronic F68 (3.0%, w/v) and chitosan (0.2%, w/v) was added to the drug/polymer mixture. The suspension was sonicated at the previously described conditions to obtain a stable formulation.

Both carriers were also synthesized without the inclusion of the drug as previously described, which may be referred to as empty nanoparticles and used as control.

2.6. Particle size, zeta potential and polydispersity index

The dynamic light scattering (DLS) technique was performed in a Nano ZS Zetasizer Instrument (Malvern Instruments Corp., UK) to determine mean size (hydrodynamic particle diameter), size distribution (polydispersity index, PDI) and Z potential (surface charge). Samples of loaded and empty nanoparticles were diluted to a final concentration of around 1.0 mg/mL and measurements

were carried out in triplicate at room temperature in polystyrene cuvettes with a path length of 10 mm using deionized water (Milli-Q system, Ma, USA).

2.7. Transmission electron microscopy (TEM)

V-NA loaded and empty formulations were analyzed under a TEM microscope (Jeol-1200 EX II, Jeol, MA, USA). For these experiments a drop of sample previously diluted ten-fold with ultrapure water was spread onto a collodion-coated Cu grid (400 mesh). After draining liquid excess with filter paper, phosphotungstic acid was added to intensify background contrast.

2.8. Analytical detection of complex

V-NA complex was quantified at λ = 332 nm by UV-Vis spectrophotometry in a microplate reader (TECAN Infinite 200 PRO, Germany). A lineal relationship was found in the range of 0-50 μM (**Figure 1S**).

2.9. Measurement of encapsulation efficiency (EE)

Calculation of EE was performed in 300 μL sample of each formulation deposited in an ultrafiltration centrifugal device (MWCO = 3000 Da, Microcon, Millipore, Ma., USA). Nanoparticles were separated from free complex by centrifugation at 10,000 ×*g*, where g is the relative centrifugal force, for 10 min and the supernatant was four times diluted in distilled water for its ulterior measurement in a UV-VIS spectrophotometry to determine encapsulation efficiency (*EE*, %) as follows:

$$EE\ (\%) = \frac{\left[Q_0 - (C_f \quad V \right.}{Q_0} \quad 100$$

where Q_0 is initial amount of V-NA complex, C_f is the final concentration of V-NA and V is the final volume after sonication.

2.10. Release studies

In vitro kinetic release of the V-NA complex from nanocarriers was performed in a 10 kDa. MWCO dialysis device (Spectra-Por® Float-ALyzer® G2, Sigma-Aldrich, Argentina) previously washed in

10% (w/v) ethanol at room temperature for 15 min. 2.0 mL-Samples of each formulation was dialyzed in a Falcon tube filled with 20.0 mL of physiological solution at pH 7.0, 37 °C and stirred at 150 rpm. Samples of 200 µL were withdrawn at defined time intervals and V-NA concentration was determined by UV-VIS spectrophotometry as mentioned before. All experiments were performed in triplicate.

2.11. Quorum sensing (QS) inhibition assay

The effect of free and nanoencapsulated V-NA complex on the production of violacein by *C. violaceum* in solid and liquid medium was evaluated because the dye production is strictly regulated by bacterial QS [35]. The surface of MH agar plates was fully inoculated with *C. violaceum,* on which 5-sterile glass cylinders were equidistantly placed and filled with 20 µL of serial dilutions of free 1.0 mM V-NA, 2,076 µM Chi/NLCs/V-NA and 949 µM Chi/Eu/V-NA. Inhibition of QS was recorded after incubation at 37 ºC for 12 h by the formation of colorless circular translucent zones around the cylinders, circumscribed by purple pigmented bacterial growth in the remaining part of the plate.

The studies of QS inhibition in liquid medium was performed by serial dilutions of the same compounds prepared in MH broth in 96-wells microtiter plates and inoculated with an inoculum of *C. violaceum* adjusted to 0.5 tube of Mc Farland scale. Plates showing bacterial growth and pigment production were visually evaluated after been incubated at 37 ºC for 24 h.

2.12. Cytotoxicity on mammalian cell cultures

Stock solutions (NLCs= 2078 µM V-NA, EuNPs= 949 µM V-NA, solvent= DMSO) were diluted to the tested concentrations directly in DMEM medium. In both cases, the range tested comprises from 1/4 to 1/32 dilutions of stock solutions (519 µM V-NA to 65 µM V-NA and 237 µM V-NA to 30µM V-NA for NLCs and EuNPs, respectively). NPs formulations were completely solubilized in aqueous or PBS mediums.

MTT [3-(4,5-dimethylthiazol-2-yl)-2,5-diphenyltetrazolium bromide] assay was used to evaluate the cytotoxicity of all compounds towards non tumoral mouse fibroblasts L929 [36]. The formation of formazan crystals from soluble tetrazolium bromide is catalyzed by a mitochondrial enzymatic complex that is only active in viable cells, assessing this way mitochondrial activity. The cell line (L929 ATCC CRL 6364 ™) was growth in Dulbecco's Modified Eagle Medium (DMEM)

supplemented with 10% Fetal Bovine serum (FBS), 100 U/mL of penicillin and 100 μg/mL of streptomycin and maintained in a humidified atmosphere with 5% CO_2 at 37 ºC. For the assays, cells seeded in 96-well plates at a density of 20,000 cells per well and incubated overnight to allow attachment were treated with serial dilutions of each compound and formulation at 37 ºC for 24 h. After treatment, the supernatant was replaced by 100 μL of MTT (0.5 mg/mL), which was discarded at 37 ºC after 3 h. Formazan crystals were solubilized with DMSO before reading the optical density at λ = 570 nm. The results, plotted as the percentage of the control value (no treatment), correspond to at least three independent experiments done with four replicates each.

2.13. Statistical analysis

Analysis of variance (ANOVA) with a significance level of 5.0% ($p < 0.05$) followed by Fisher's least significant difference test ($p < 0.05$) was selected for comparisons of the means. All values were reported as the mean and standard deviation of two or three independent experiments.

3. Results and discussion

3.1. Evaluation of the antimicrobial properties of the V-NA complex

The ability of the complex V-NA to inhibit Gram (+) and Gram (-) strains was determined by broth microdilution method and the resulting MIC and IC_{50} values were compared with the NA ligand (**Table 1** and **Figure 2S**). The antimicrobial activity of V-NA complex was remarkably higher than that of NA, since a two-fold reduction ratio of MIC and IC_{50} values against all strains was observed. A strong inhibition against *E. Coli* and *B. cereus* was produced, with MIC values of 10 μM for both strains. However, both compounds have a weaker antibacterial activity against biofilm forming strains like *P. aeruginosa* and *S. aureus* with MIC values of 625 μg/mL and 125 μg/mL respectively. For therapeutic purposes those high MIC values could produce undesirable side effects on mammalian cells and tissues and, consequently, an improvement in the antimicrobial activity would be necessary.

In addition, the enhanced activity of the complex in comparison with NA was demonstrated by antibiogram assay (**Figure 1**). An increase in the inhibition halo was mainly observed against *P. aeruginosa* and *S. aureus* for both compounds at the concentration of 10 mM. No differences were found for *E. Coli* and *B. cereus* possible due to the higher susceptibility to the antimicrobials at that

concentration. However, clear differences were elucidated against the four strains at a concentration 100 times lower. A halo increase in the range of 46-65 % was found when V-NA was compared with NA, suggesting a potentiation of the antibiotic activity in the complexed form.

The effectiveness of the antibacterial potential of V-NA versus NA was also *in-situ* studied by fluorescence microscopy using Live/Dead BacLight® kit (**Figure 2**). Treatments with NA showed that the green fluorescence prevails in the Live channel, indicating the presence of viable bacteria. By the other side, the prevalence of red stained cells suggests the presence of death bacteria in the DEAD channel mainly derived from the treatment with 100 μg/mL V-NA for 1 hour. The merged images displayed the high biocidal activity of the V-NA complex compared to NA and mainly observed in the case of *E. Coli,* and in less extent against *S. aureus* and *B. cereus.* The differences were not significant in *P. aeruginosa*, since the MIC value was not reach and no dead of the bacteria was observed.

Finally, TEM images of the different stains treated with V-NA at concentrations two-times higher than their respective MICs were obtained (**Figure 3**). No noticeable morphological changes in bacterial cells after their exposure to the V-NA complex were elucidated, suggesting that its action mechanism is more associated with metabolic inhibition than membrane targeting. This is logical considering that NA is a synthetic quinolone drug class and the main target is the microbial topoisomerase type II (*i.e.* DNA gyrase), while vanadium(IV) activity could induce intracellular oxygen reactive species and inactivation of some DNA-metabolizing enzymes [37,38].

The V-NA complex appears to have a bacteriostatic effect against all strains, since MBCs for *E. coli, B. Cereus* and *S. aureus* were five or more dilutions greater than their corresponding MICs. Furthermore, the MBC towards *P. aeruginosa* was over 5,000 μM (**Table 2**).

3.2. Swarming motility inhibition by V-NA

The major role of *swarming* motility is surface colonization and subsequent formation of biofilms, which are one of the main forms of bacterial growth and one of the greatest obstacles for the treatment of microbial pathogens [39]. On the other hand, *swarming* has been directly associated with virulence and antibiotic resistance in some microorganisms including *P. aeruginosa* [40,41]. A considerable reduction of swarming motility is observed in *S. aureus* and *P. aeruginosa* strains when treated with

sub-inhibitory concentrations of the V-NA complex, from 2.5 to 10 times less than their corresponding CIM value at 1, 2 and 7 days. Also, the inhibitory effect is more evident on *P. aeruginosa* a very promiscuous pathogen in mammals (**Figure 3**). Interestingly, the reduction of swarming motility in presence of sub-inhibitory concentrations of the complex could imply a decrease of pathogenic potential of the microbial strains, thus probably affect the development of infection in a host [42].

3.3. Synthesis and characterization of NLCs and EuNPs for V-NA encapsulation

Despite the potentiation of the antimicrobial activity of NA by complexation with vanadium was demonstrated in the previous experiments, a weak antibacterial activity was observed against two biofilm forming strains: *P. aeruginosa* and *S. aureus*. In this sense, nanoencapsulation in NLCs and EuNPs was proposed as an alternative to improve the antimicrobial activity of V-NA and to increase its bioavailability.

The ultrasonication method was successfully applied for the preparation of stable formulations of Chi-coated NLCs and EuNPs. TEM analysis of empty formulations revealed spherically shaped particles, whose morphology did not show any changes after the encapsulation of the complex (**Figure 4**). The particle sizes were in the nanometric range with an excellent homogeneity and absence of aggregates. In concordance, the DLS analyses showed that empty and loaded polymeric nanoparticles exhibited mean sizes of 198.0±1.4 nm and 168.4±1.5 nm for EuNPs respectively **(Table 3**). Particle sizes obtained for NLCs were around 236.9±2.2 nm to 331.6±5.1 nm for empty and loaded NPs respectively. Interaction of the cargo molecules with the matrices could produce changes in the viscosity of the mixtures [43]. At low viscosities of the raw materials, smaller nanoparticles could be obtained by hot-homogenization method. This phenomenon suggests that V-NA could be stronger interacting with the polymeric matrix than with the lipidic matrix. For that reason, smaller NPs were obtained when V-NA was encapsulated into EuNPs. It is important to observe that EuNPs showed mean diameters significantly smaller than NLCs ($p<0.05$).

PDI values showed that monodispersed nanoparticles were obtained and the Z potential data from +11 to +30 mV demonstrated a positive surface charge for all the samples that could be adjudicated to positively charged chitosan adsorbed in the surface of nanoparticles [20].

The main intended administration route for the present nanoparticles is the parenteral. A rapid antimicrobial response is expected after nanoparticles directly reached the systemic circulation. Different articles suggest the use of similar nanoparticles via *i.v.* administration to enhance the properties of the delivered drugs. NLCs, chitosan, solid lipid or polymeric nanoparticles probe to be effective carriers for antibiotics, antithumoral or antivirals [44–48]. An alternative less-invasive route of administration for the nanoparticles developed in our work could be pulmonary delivery. The stability of the solutions makes them suitable candidates to be nebulized and reach the deepest interstices of the pulmonary system in the treatment of severe infections. High drug permeability could be produced due to the large surface area of lung [20,49]. According to those statements, the release experiments were performed in physiological solution at pH 7.0 and 37ºC to evaluate the V-NA concentrations obtained in time.

V-NA was encapsulated with excellent efficiency in both formulations displaying 97.8±0.5% EE for NLCs and 96.1±0.1% for EuNPs. In addition, both formulations of V-NA displayed a steadily release according to the kinetic profiles (**Figure 5**). Interestingly, both nanosystems exhibited biphasic *in vitro* release patterns, as could be envisaged on the basis of previous reports [21]. The release kinetic is directly associated with stability and therapeutic results of a drug [50].

The NLCs showed a reduced release profile of V-NA than the observed for EuNPs. This behavior could be attributed to the higher size of NLCs nanoparticles in comparison with EuNPs with values of 331.6±5.1 and 168.4±1.5 respectively. The drug release is especially affected by particle diameter, which is in close relationship with the surface area-to-volume ratio. In this sense, smaller NPs show a higher specific surface and therefore, a larger amount of the drug will be close to the surrounded media leading to a faster drug release [22]. Considering that EuNPs have a surface area-to-volume ratio 1.97 higher than the ratio of NLCs, a higher amount of drug released is expected.

The initial burst release elucidated in both systems could be mainly attributed to desorption of the surface-bound or adsorbed drug on the surface of nanoparticles. The carriers released the complex in a sustained manner, reaching 30-40% released drug percentage after a 48 h period. A brief comparison with other works that reported the release of quinolones, revealed that V-NA was delivered in a controlled way from those systems. Rodenak *et al*. described the release of Ofloxacin from chitosan/SLN reaching an 80-95% of the drug in 24 hours [20]. The release of methazolamide from a similar delivery system showed a burst release of the drug with 100% in 8 hours [51]. A slower profile was observed for carbamazepine with a 30-70% release of the drug in 24 hours with different compositions of chitosan-coated SLN [52].

Vehiculization into hybrid NPs provides advantages such as the increased solubility and controlled release of the V-NA. Nalidixic acid is poorly soluble inwater (0.1 mg/mL at 23 °C, XLogP3= 1.4) as well as the V-NA complex. Nanoencapsulation into colloidal systems increases the solubility in physiological media. Stable formulation of NLCs and EuNPs containing 1 mg/mL of the V-NA are obtained at room temperature and still remain stable at 5°C under storage for at least 3 months. Also, the presence of chitosan would play a key role in NPs stabilization, controlled release of the drug and binding to the bacterial surface [20].

3.4. Antimicrobial evaluation of V-NA loaded NLCs and EuNP formulations

V-NA vehiculization into nanoparticles proved to be an effective tool for enhancing its antimicrobial activity (**Figure 6**). Despite the MIC of V-NA loaded NLCs against *S. aureus* was in the same order than V-NA (129.9 vs. 125 µM), a considerable effectiveness was observed for EuNPs (59.3 µM) displaying a MIC reduction of at least two-times than the free complex. More interesting was the effect on *P. aeruginosa*, since V-NA loaded NLCs and V-NA loaded EuNPs formulations showed a five-fold (129.9 µM) and a ten-fold (59.3 µM) MIC reduction respectively, compared to the V-NA. These results are strongly suggesting that V-NA loaded EuNPs formulation would be the most effective from the tested systems to inhibit *P. aeruginosa* and *S. aureus* growth.

Previous work from our laboratory demonstrated that chitosan plays a key role in providing positive nanoparticles with enhanced mucoadhesivity. In this sense, and considering the negative surface of the bacteria membrane, a strong electrostatic interaction could be established between the hybrid NP and the bacteria. This close contact allows NP to release the antibiotic in a site-specific way, which clearly increases the bioavailability of the drug and the antimicrobial effect [20]. In addition, the effect of membrane destabilization by the presence of chitosan on NP surface will be contributing to the bacterial damage [53].

3.5. Quorum sensing inhibition

Swimming and twitching motilities involve individual independent cellular movement, while swarming requires effective bacterial communication through *QS* system [39].
Considering the close relation between both phenomena, the effect of free and encapsulated V-NA in NLCs and EuNPs on *QS* was evaluated by violacein produced by *C. violaceum*. That strain was selected as reporter microorganism since it is a reference to check the presence of QS molecules. The production of a violet pigment is the result of QS interactions between the bacterial cells. In this sense, inhibition of pigment production could be attributed to inhibition of QS mechanism as was suggested in different works [54,55].

Both nanoparticle formulations showed QS inhibition (QSI) activity, which is evidenced by the loss of pigmentation of *C. Violaceum* and the resulting white colored, opaque zones with intact bacteria (**Figure 7I**). On the other side, free V-NA complex produced growth inhibition zones but had no effect on violacein production, suggesting an important role of NPs in interfering with QS communication (**Figure 7II** and **7III**). Violacein production could be observed on column H, though a less intensity was observed in presence of V-NA loaded NLCs and EuNPs than the control. After revealing the plates with resazurin, the results indicated the presence of V-NA loaded nanoparticles inhibiting QS, as it was revealed by bacterial growth in wells where violacein production was repressed (**Figure 7, Column G**).

3.6. Cell cytotoxicity

The toxicity profile of NA, V-NA, V-NA loaded NLCs and V-NA loaded EuNPs was evaluated on L929 cells by viability assay using the MTT method. The L929 cells were used since it is the reference cell strain that ATCC recommend to use for cell toxicity test. In addition, L929 cells were commonly used to test the *in vitro* cytocompatibility of different types of nanoparticles [56,57].

A decrease in cell viability inhibition of V-NA in the range of 10-500 μM in comparison with free NA was observed. However, the deleterious effect of free NA and V-NA is not pronounced since cell viability remains above 50% even at concentrations up to 500 μM (**Figure 8**). Moreover, the empty Eudragit and NLCs formulations did not show that exert cytotoxicity on L929 cells at dilution factors in the range of 4 to 32 (data not shown).

Regarding the encapsulated V-NA complex, Eudragit formulation was found to have a lower cytotoxicity effect than its NLCs counterpart (**Figure 9**). It is important to highlight that V-NA-Eudragit nanoparticle did not show deleterious effect on L929 cells from 30 to 240 μM with cell viability percentages higher than 70%. Nevertheless, in those range of concentrations, Eudragit nanoformulation showed an effective antibacterial activity against *P. aeruginosa* and *S. aureus* (CIM = 59.3 μM). These results are very relevant since the use of Eudragit nanoformulation improve the antibacterial effects of V-NA complex without altering the cytotoxicity on normal cells showing a pharmacological selectivity. In this order, Graça and coworkers reported that different Eudragit nanosystems did not display cytotoxic effects on L929 cells [58]. Finally, the NLCs formulation show a cell toxicity in the limit of the observed MIC for *P. aeruginosa* and *S. aureus,* since at the concentration of 130 μM V-NA, the cell viability was reduced around 30%.

Conclusions

Nanoencapsulated nalidixic acid-vanadium complex

In the present work, the antibacterial activity of an oxidovanadium(IV)-nalidixato complex (V-NA) has been substantially enhanced after its successful encapsulation in Chi coated NLCs and EuNPs. The vehiculization of the V-NA complex into chitosan-based nanoparticles proved an effective approach to increase its antimicrobial activity and also to have an inhibitory effect on QS observed by the violacein production by *C. violaceum.* Cytocompatibility studies revealed the low cytotoxicity of all tested nanosystems on mammalian cells and V-NA loaded EuNPs seems to be the most suitable system for potential pharmaceutical applications on considering its low toxicity against L929 cells. Taking in account the world's global context of pandemics associated to bacteria and virus, the obtained results highlight a potential therapeutic system for infectious diseases. Future studies need to be carried out with multidrug-resistant microorganism isolated from clinical patients and testing V-NA loaded NPs in proper animal models for pre-clinical studies is essential.

Acknowledgments

This work was supported by UNLP (X041), CONICET (PIP 0034-PIP 0498), and ANPCyT (PICT 2016-1574, PICT 2017-2251). IEL, GAI, and GRC are members of the Carrera del Investigador, CONICET, Argentina. EG and DS thank Regione Autonoma della Sardegna (grant RASSR79857) for financial support. Also, we really appreciate the donation of Eudragit® samples to Etilfarma® (Buenos Aires, Argentina) and CRODA® Argentina for kindly donating the lipids.

All authors have no Conflicts of Interest.

References

[1] N. Cassir, J.M. Rolain, P. Brouqui, A new strategy to fight antimicrobial resistance: The revival of old antibiotics, Front. Microbiol. 5 (2014). https://doi.org/10.3389/fmicb.2014.00551.

[2] M. Saddam Hossain, Metal Complexes as Potential Antimicrobial Agent: A Review, Am. J. Heterocycl. Chem. 4 (2018) 1. https://doi.org/10.11648/j.ajhc.20180401.11.

[3] L. Giovagnini, S. Sitran, M. Montopoli, L. Caparrotta, M. Corsini, C. Rosani, P. Zanello, Q.P. Dou, D. Fregona, Chemical and biological profiles of novel copper(II) complexes containing S-donor ligands for the treatment of cancer, Inorg. Chem. 47 (2008) 6336–6343. https://doi.org/10.1021/ic800404e.

[4] K.H. Thompson, C. Orvig, Vanadium in diabetes: 100 years from Phase 0 to Phase I, J. Inorg. Biochem. 100 (2006) 1925–1935. https://doi.org/10.1016/j.jinorgbio.2006.08.016.

[5] S.I. Pillai, S.P. Subramanian, M. Kandaswamy, A novel insulin mimetic vanadium-flavonol complex: Synthesis, characterization and in vivo evaluation in STZ-induced rats, Eur. J. Med. Chem. 63 (2013) 109–117. https://doi.org/10.1016/j.ejmech.2013.02.002.

[6] A.M. Cortizo, M.S. Molinuevo, D.A. Barrio, L. Bruzzone, Osteogenic activity of vanadyl(IV)-ascorbate complex: Evaluation of its mechanism of action, Int. J. Biochem. Cell Biol. 38 (2006) 1171–1180. https://doi.org/10.1016/j.biocel.2005.12.007.

[7] M. Fernández, J. Varela, I. Correia, E. Birriel, J. Castiglioni, V. Moreno, J. Costa Pessoa, H. Cerecetto, M. González, D. Gambino, A new series of heteroleptic oxidovanadium(iv) compounds with phenanthroline-derived co-ligands: Selective Trypanosoma cruzi growth inhibitors, Dalt. Trans. 42 (2013) 11900–11911. https://doi.org/10.1039/c3dt50512j.

[8] D. Rehder, Perspectives for vanadium in health issues, Future Med. Chem. 8 (2016) 325–338. https://doi.org/10.4155/fmc.15.187.

[9] E. Kioseoglou, S. Petanidis, C. Gabriel, A. Salifoglou, The chemistry and biology of vanadium compounds in cancer therapeutics, Coord. Chem. Rev. 301–302 (2015) 87–105. https://doi.org/10.1016/j.ccr.2015.03.010.

[10] D.C. Crans, L.R. Henry, G. Cardiff, B.I. Posner, Developing Vanadium as an Antidiabetic or Anticancer Drug: A Clinical and Historical Perspective, Met. Ions Life Sci. 19 (2019). https://doi.org/10.1515/9783110527872-014.

[11] I. Leon, J. Cadavid-Vargas, A. Di Virgilio, S. Etcheverry, Vanadium, Ruthenium and Copper

Compounds: A New Class of Nonplatinum Metallodrugs with Anticancer Activity, Curr. Med. Chem. (2016). https://doi.org/10.2174/0929867323666160824162546.

[12] J.C. Pessoa, S. Etcheverry, D. Gambino, Vanadium compounds in medicine, Coord. Chem. Rev. 301–302 (2015) 24–48. https://doi.org/10.1016/j.ccr.2014.12.002.

[13] M.J. Hosseini, F. Shaki, M. Ghazi-Khansari, J. Pourahmad, Toxicity of vanadium on isolated rat liver mitochondria: A new mechanistic approach, Metallomics. 5 (2013) 152–166. https://doi.org/10.1039/c2mt20198d.

[14] A. Wilk, D. Szypulska-Koziarska, B. Wiszniewska, The toxicity of vanadium on gastrointestinal, urinary and reproductive system, and its influence on fertility and fetuses malformations, Postepy Hig. Med. Dosw. (Online). 71 (2017) 850–859. https://doi.org/10.5604/01.3001.0010.4783.

[15] O.I. Fatola, F.A. Olaolorun, F.E. Olopade, J.O. Olopade, Trends in vanadium neurotoxicity, Brain Res. Bull. 145 (2019) 75–80. https://doi.org/10.1016/j.brainresbull.2018.03.010.

[16] M. Ochubiojo, I. Chinwude, E. Ibanga, S. Ifianyi, Nanotechnology in Drug Delivery, in: Recent Adv. Nov. Drug Carr. Syst., 2012. https://doi.org/10.5772/51384.

[17] R. Cortesi, G. Valacchi, X.M. Muresan, M. Drechsler, C. Contado, E. Esposito, A. Grandini, A. Guerrini, G. Forlani, G. Sacchetti, Nanostructured lipid carriers (NLC) for the delivery of natural molecules with antimicrobial activity: production, characterization and *in vitro* studies, J. Microencapsul. 0 (2017) 1–33. https://doi.org/10.1080/02652048.2017.1284276.

[18] L. Sercombe, T. Veerati, F. Moheimani, S.Y. Wu, A.K. Sood, S. Hua, Advances and challenges of liposome assisted drug delivery, Front. Pharmacol. 6 (2015). https://doi.org/10.3389/fphar.2015.00286.

[19] G.A. Islan, M.L. Cacicedo, B. Rodenak-Kladniew, N. Duran, G.R. Castro, Development and Tailoring of Hybrid Lipid Nanocarriers, Curr. Pharm. Des. 23 (2018) 6643–6658. https://doi.org/10.2174/1381612823666171115110639.

[20] B. Rodenak-Kladniew, S.S. Montoto, M.L. Sbaraglini, M. Di Ianni, M.E. Ruiz, A. Talevi, V.A. Alvarez, N. Durán, G.R. Castro, G.A. Islan, Hybrid Ofloxacin/eugenol co-loaded solid lipid nanoparticles with enhanced and targetable antimicrobial properties, Int. J. Pharm. 569 (2019) 118575. https://doi.org/10.1016/j.ijpharm.2019.118575.

[21] G.A. Islan, P.C. Tornello, G.A. Abraham, N. Duran, G.R. Castro, Smart lipid nanoparticles containing levofloxacin and DNase for lung delivery. Design and characterization, Colloids Surfaces B Biointerfaces. 143 (2016) 168–176. https://doi.org/10.1016/j.colsurfb.2016.03.040.

[22] P.N. Navya, H.K. Daima, Rational engineering of physicochemical properties of nanomaterials for biomedical applications with nanotoxicological perspectives, Nano Converg. 3 (2016). https://doi.org/10.1186/s40580-016-0064-z.

[23] W.J. Lin, Y.S. Duh, Nanostructured lipid carriers for transdermal delivery of acid labile lansoprazole, Eur. J. Pharm. Biopharm. 108 (2016) 297–303. https://doi.org/10.1016/j.ejpb.2016.07.015.

[24] G. Yoon, J.W. Park, I.-S. Yoon, Solid lipid nanoparticles (SLNs) and nanostructured lipid carriers (NLCs): recent advances in drug delivery, J. Pharm. Investig. 43 (2013) 353–362. https://doi.org/10.1007/s40005-013-0087-y.

[25] P. Ghasemiyeh, S. Mohammadi-Samani, Solid lipid nanoparticles and nanostructured lipid carriers as novel drug delivery systems: Applications, advantages and disadvantages, Res. Pharm. Sci. 13 (2018) 288–303. https://doi.org/10.4103/1735-5362.235156.

[26] J. Han, D. Zhao, D. Li, X. Wang, Z. Jin, K. Zhao, Polymer-based nanomaterials and applications for vaccines and drugs, Polymers (Basel). 10 (2018). https://doi.org/10.3390/polym10010031.

[27] G. Sandri, S. Motta, M.C. Bonferoni, P. Brocca, S. Rossi, F. Ferrari, V. Rondelli, L. Cantù, C. Caramella, E. Del Favero, Chitosan-coupled solid lipid nanoparticles: Tuning nanostructure and mucoadhesion, Eur. J. Pharm. Biopharm. 110 (2017) 13–18.

https://doi.org/10.1016/j.ejpb.2016.10.010.

[28] Y. El-Malah, S. Nazzal, Novel use of Eudragit® NE 30D/Eudragit® L 30D-55 blends as functional coating materials in time-delayed drug release applications, Int. J. Pharm. 357 (2008) 219–227. https://doi.org/10.1016/j.ijpharm.2008.02.003.

[29] D. Sanna, V. Ugone, G. Sciortino, P. Buglyó, Z. Bihari, P.L. Parajdi-Losonczi, E. Garribba, VIVO complexes with antibacterial quinolone ligands and their interaction with serum proteins, Dalt. Trans. 47 (2018) 2164–2182. https://doi.org/10.1039/c7dt04216g.

[30] M. Kresken, B. Wiedemann, Development of resistance to nalidixic acid and the fluoroquinolones after the introduction of norfloxacin and ofloxacin, Antimicrob. Agents Chemother. 32 (1988) 1285–1288. https://doi.org/10.1128/AAC.32.8.1285.

[31] D.F. Evans, P.H. Missen, Water-soluble Schiff-base complexes of vanadyl(IV) and vanadium(III), J. Chem. Soc. Dalt. Trans. (1987) 1279–1281. https://doi.org/10.1039/DT9870001279.

[32] A. Tarushi, P. Christofis, G. Psomas, Synthesis, characterization and interaction with DNA of mononuclear metal complexes with oxolinic acid, Polyhedron. 26 (2007) 3963–3972. https://doi.org/10.1016/j.poly.2007.04.031.

[33] S.D. Sarker, L. Nahar, Y. Kumarasamy, Microtitre plate-based antibacterial assay incorporating resazurin as an indicator of cell growth, and its application in the in vitro antibacterial screening of phytochemicals, Methods. (2007). https://doi.org/10.1016/j.ymeth.2007.01.006.

[34] G.A. Islan, M.E. Ruiz, J.F. Morales, M.L. Sbaraglini, A.V. Enrique, G. Burton, A. Talevi, L.E. Bruno-Blanch, G.R. Castro, Hybrid inhalable microparticles for dual controlled release of levofloxacin and DNase: Physicochemical characterization and in vivo targeted delivery to the lungs, J. Mater. Chem. B. 5 (2017) 3132--3144. https://doi.org/10.1039/c6tb03366k.

[35] K.H. McClean, M.K. Winson, L. Fish, A. Taylor, S.R. Chhabra, M. Camara, M. Daykin, J.H.

Lamb, S. Swift, B.W. Bycroft, G.S.A.B. Stewart, P. Williams, Quorum sensing and Chromobacterium violaceum: Exploitation of violacein production and inhibition for the detection of N-acylhomoserine lactones, Microbiology. 143 (1997) 3703–3711. https://doi.org/10.1099/00221287-143-12-3703.

[36] T. Mosmann, Rapid colorimetric assay for cellular growth and survival: Application to proliferation and cytotoxicity assays, J. Immunol. Methods. 65 (1983) 55–63. https://doi.org/10.1016/0022-1759(83)90303-4.

[37] J. Wang, H. Zhou, G. Guo, T. Cheng, X. Peng, X. Mao, J. Li, X. Zhang, A functionalized surface modification with vanadium nanoparticles of various valences against implant-associated bloodstream infection, Int. J. Nanomedicine. 12 (2017) 3121–3136. https://doi.org/10.2147/IJN.S129459.

[38] M. Pisano, C. Arru, M. Serra, G. Galleri, D. Sanna, E. Garribba, G. Palmieri, C. Rozzo, Antiproliferative activity of vanadium compounds: Effects on the major malignant melanoma molecular pathways, Metallomics. 11 (2019) 1687–1699. https://doi.org/10.1039/c9mt00174c.

[39] C. O'May, N. Tufenkji, The swarming motility of Pseudomonas aeruginosa is blocked by cranberry proanthocyanidins and other tannin-containing materials, Appl. Environ. Microbiol. 77 (2011) 3061–3067. https://doi.org/10.1128/AEM.02677-10.

[40] R.M. Harshey, Bacterial Motility on a Surface: Many Ways to a Common Goal, Annu. Rev. Microbiol. 57 (2003) 249–273. https://doi.org/10.1146/annurev.micro.57.030502.091014.

[41] T. Inoue, R. Shingaki, K. Fukui, Inhibition of swarming motility of Pseudomonas aeruginosa by branched-chain fatty acids, FEMS Microbiol. Lett. 281 (2008) 81–86. https://doi.org/10.1111/j.1574-6968.2008.01089.x.

[42] S. Rütschlin, T. Böttcher, Inhibitors of Bacterial Swarming Behavior, Chem. - A Eur. J. 26 (2020) 964–979. https://doi.org/10.1002/chem.201901961.

[43] V.E. Bosio, A.G. López, A. Mukherjee, M. Mechetti, G.R. Castro, Tailoring doxorubicin

sustainable release from biopolymeric smart matrix using congo red as molecular helper, J. Mater. Chem. B. 2 (2014) 5178–5186. https://doi.org/10.1039/c3tb20531b.

[44] J. - C Leroux, E. Doelker, R. Gurny, R. Cozens, J.L. Roesel, B. Galli, F. Kubel, Pharmacokinetics of a novel HIV- 1 protease inhibitor incorporated into biodegradable or enteric nanoparticles following intravenous and oral administration to mice, J. Pharm. Sci. 84 (1995) 1387–1391. https://doi.org/10.1002/jps.2600841202.

[45] K. Manjunath, V. Venkateswarlu, Pharmacokinetics, tissue distribution and bioavailability of clozapine solid lipid nanoparticles after intravenous and intraduodenal administration, J. Control. Release. 107 (2005) 215–228. https://doi.org/10.1016/j.jconrel.2005.06.006.

[46] L. Qi, Z. Xu, In vivo antitumor activity of chitosan nanoparticles, Bioorganic Med. Chem. Lett. 16 (2006) 4243–4245. https://doi.org/10.1016/j.bmcl.2006.05.078.

[47] M. Fazil, S. Md, S. Haque, M. Kumar, S. Baboota, J.K. Sahni, J. Ali, Development and evaluation of rivastigmine loaded chitosan nanoparticles for brain targeting, Eur. J. Pharm. Sci. 47 (2012) 6–15. https://doi.org/10.1016/j.ejps.2012.04.013.

[48] A. Beloqui, M.A. Solinís, A. Delgado, C. Évora, A. Del Pozo-Rodríguez, A. Rodríguez-Gascón, Biodistribution of Nanostructured Lipid Carriers (NLCs) after intravenous administration to rats: Influence of technological factors, Eur. J. Pharm. Biopharm. 84 (2013) 309–314. https://doi.org/10.1016/j.ejpb.2013.01.029.

[49] O. Taratula, A. Kuzmov, M. Shah, O.B. Garbuzenko, T. Minko, Nanostructured lipid carriers as multifunctional nanomedicine platform for pulmonary co-delivery of anticancer drugs and siRNA, J. Control. Release. 171 (2013) 349–357. https://doi.org/10.1016/j.jconrel.2013.04.018.

[50] X.Y. Lu, D.C. Wu, Z.J. Li, G.Q. Chen, Polymer nanoparticles, in: Prog. Mol. Biol. Transl. Sci., 2011: pp. 299–323. https://doi.org/10.1016/B978-0-12-416020-0.00007-3.

[51] F. Wang, M. Zhang, D. Zhang, Y. Huang, L. Chen, S. Jiang, K. Shi, R. Li, Preparation,

optimization, and characterization of chitosan-coated solid lipid nanoparticles for ocular drug delivery, J. Biomed. Res. 32 (2018) 411–423. https://doi.org/10.7555/JBR.32.20160170.

[52] R. Nair, A.C. Kumar, V.K. Priya, C.M. Yadav, P.Y. Raju, Formulation and evaluation of chitosan solid lipid nanoparticles of carbamazepine, Lipids Health Dis. 11 (2012). https://doi.org/10.1186/1476-511X-11-72.

[53] M. Kong, X.G. Chen, K. Xing, H.J. Park, Antimicrobial properties of chitosan and mode of action: A state of the art review, Int. J. Food Microbiol. 144 (2010) 51–63. https://doi.org/10.1016/j.ijfoodmicro.2010.09.012.

[54] D. Martinelli, G. Grossmann, U. Séquin, H. Brandl, R. Bachofen, Effects of natural and chemically synthesized furanones on quorum sensing in Chromobacterium violaceum, BMC Microbiol. 4 (2004). https://doi.org/10.1186/1471-2180-4-25.

[55] S.A. Burt, V.T.A. Ojo-Fakunle, J. Woertman, E.J.A. Veldhuizen, The natural antimicrobial carvacrol inhibits quorum sensing in chromobacterium violaceum and reduces bacterial biofilm formation at sub-lethal concentrations, PLoS One. 9 (2014). https://doi.org/10.1371/journal.pone.0093414.

[56] H. Atalay, A. Çelik, F. Ayaz, Investigation of genotoxic and apoptotic effects of zirconium oxide nanoparticles (20 nm) on L929 mouse fibroblast cell line, Chem. Biol. Interact. 296 (2018) 98–104. https://doi.org/10.1016/j.cbi.2018.09.017.

[57] K. Kanimozhi, S.K. Basha, K. Kaviyarasu, V. SuganthaKumari, Salt Leaching Synthesis, Characterization and In Vitro Cytocompatibility of Chitosan/Poly(vinyl alcohol)/Methylcellulose – ZnO Nanocomposites Scaffolds Using L929 Fibroblast Cells , J. Nanosci. Nanotechnol. 19 (2019) 4447–4457. https://doi.org/10.1166/jnn.2019.16359.

[58] D. Graça, H. Louro, J. Santos, K. Dias, A.J. Almeida, L. Gonçalves, M.J. Silva, A. Bettencourt, Toxicity screening of a novel poly(methylmethacrylate)-Eudragit nanocarrier on L929 fibroblasts, Toxicol. Lett. 276 (2017) 129–137.

https://doi.org/10.1016/j.toxlet.2017.05.017.

Figures

Figure 1 Antibiogram of NA and V-NA complex at two concentrations against different strains.

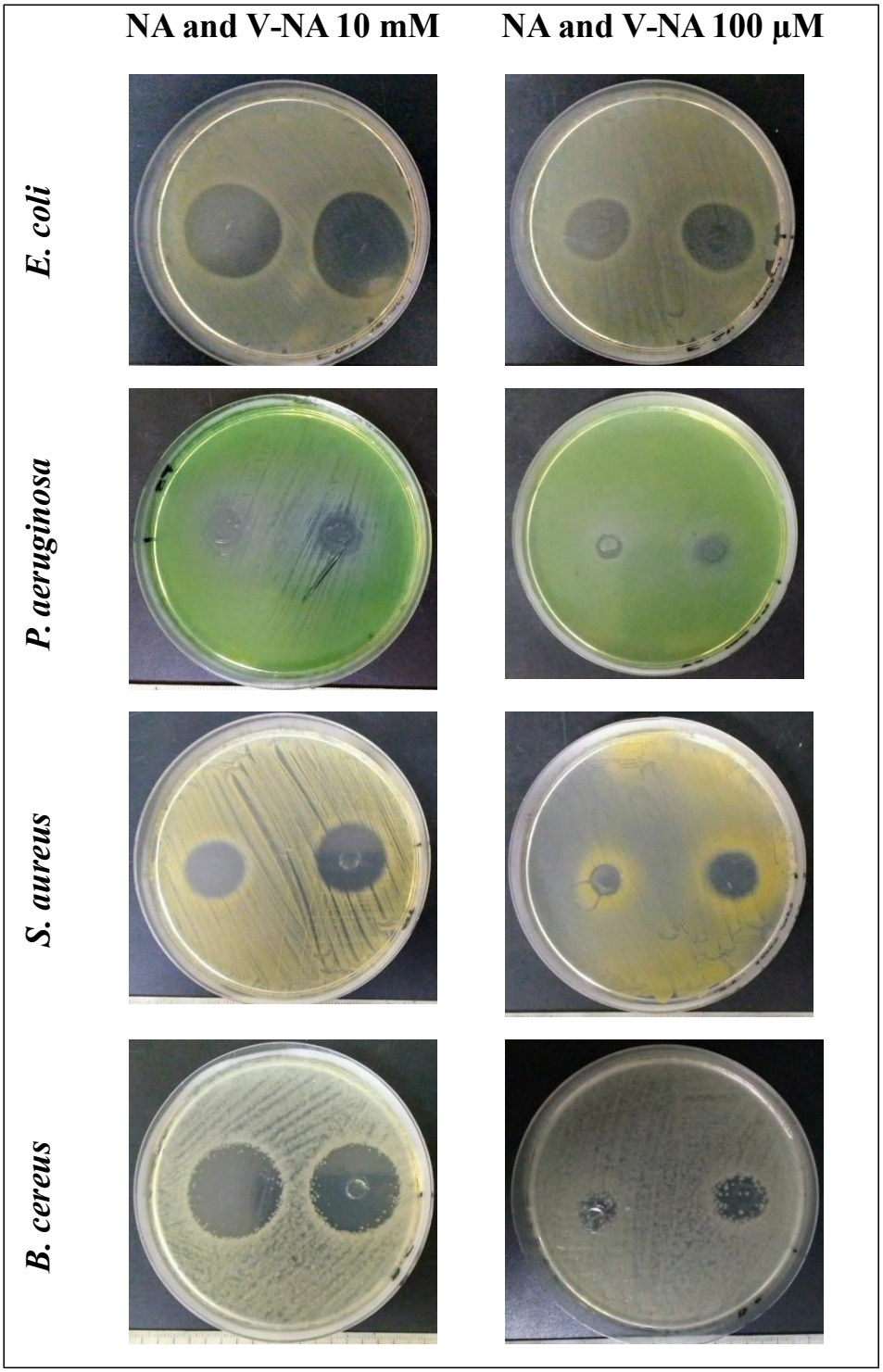

Figure 2. Representative epifluorescence microscope images of *Escherichia coli*, *Staphylococcus aureus, Bacillus cereus* and *Pseudomonas aeruginosa* planktonic cells stained with the Live/Dead BacLight® kit. LIVE and DEAD channels are used to observe the samples subjected to a one-hour treatment with NA (100 µM) or V-NA (100 µM).

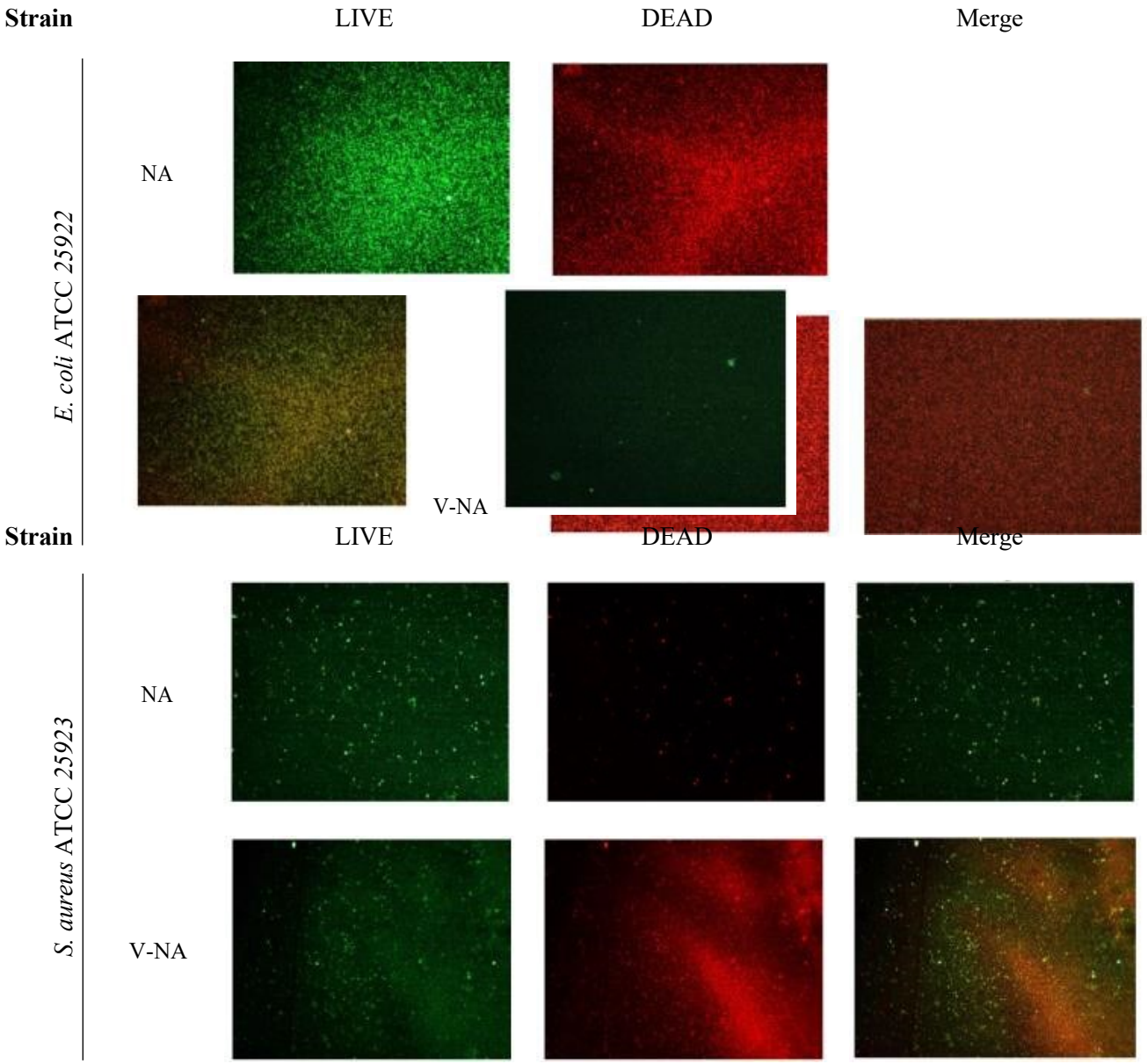

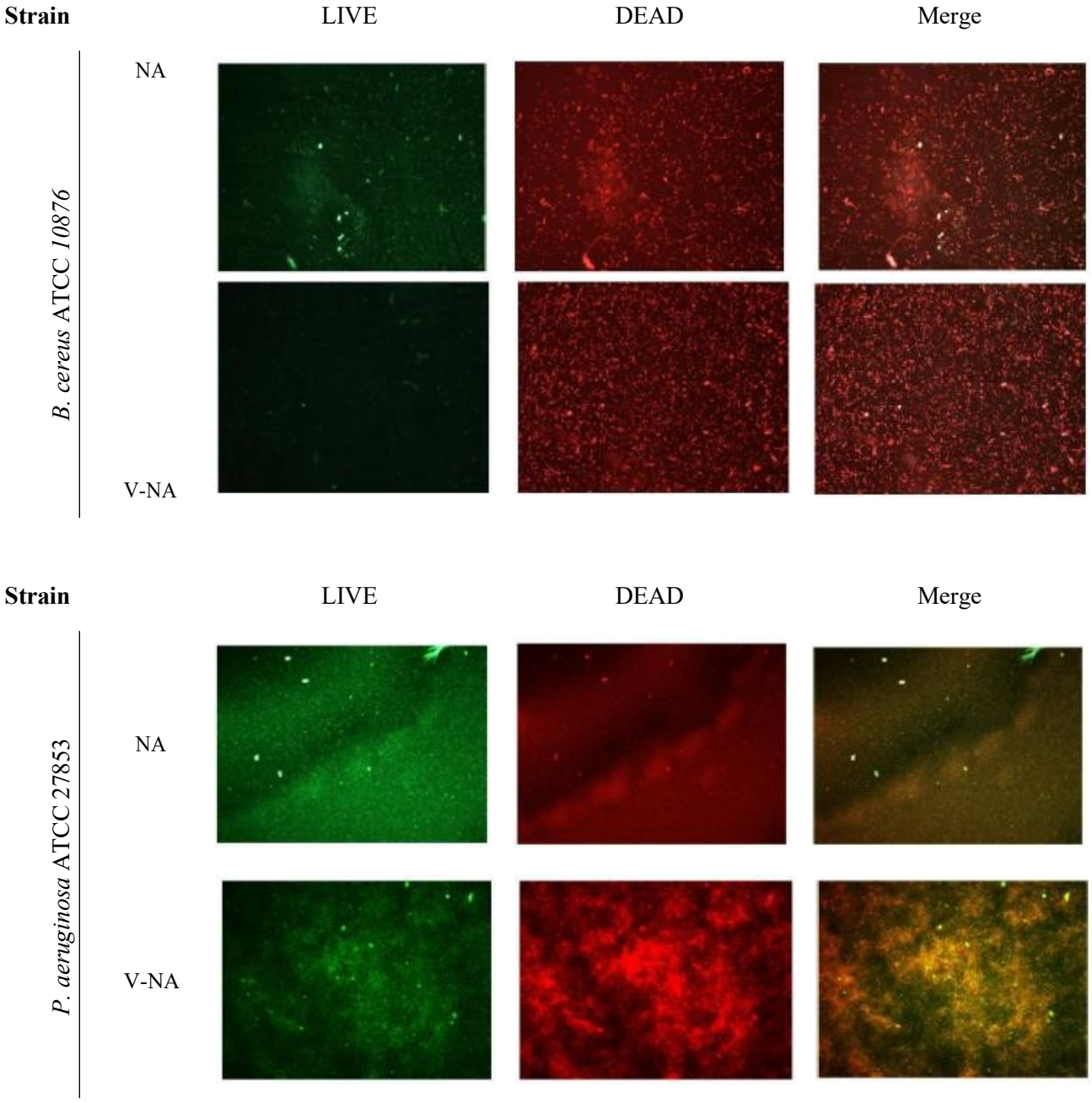
Strain
LIVE
DEAD
Merge
B. cereus ATCC 10876
NA
V-NA
Strain
LIVE
DEAD
Merge
P. aeruginosa ATCC 27853
NA
V-NA

Figure 3. Swarming inhibition assay. Graphs depict the data taken from the photographs of *P. aeruginosa* (top) and *S. aureus* (bottom) seeded in agar 0.4 wt% plates supplemented with the V-NA at 50 µM, after 1, 2 and 7 days incubation.

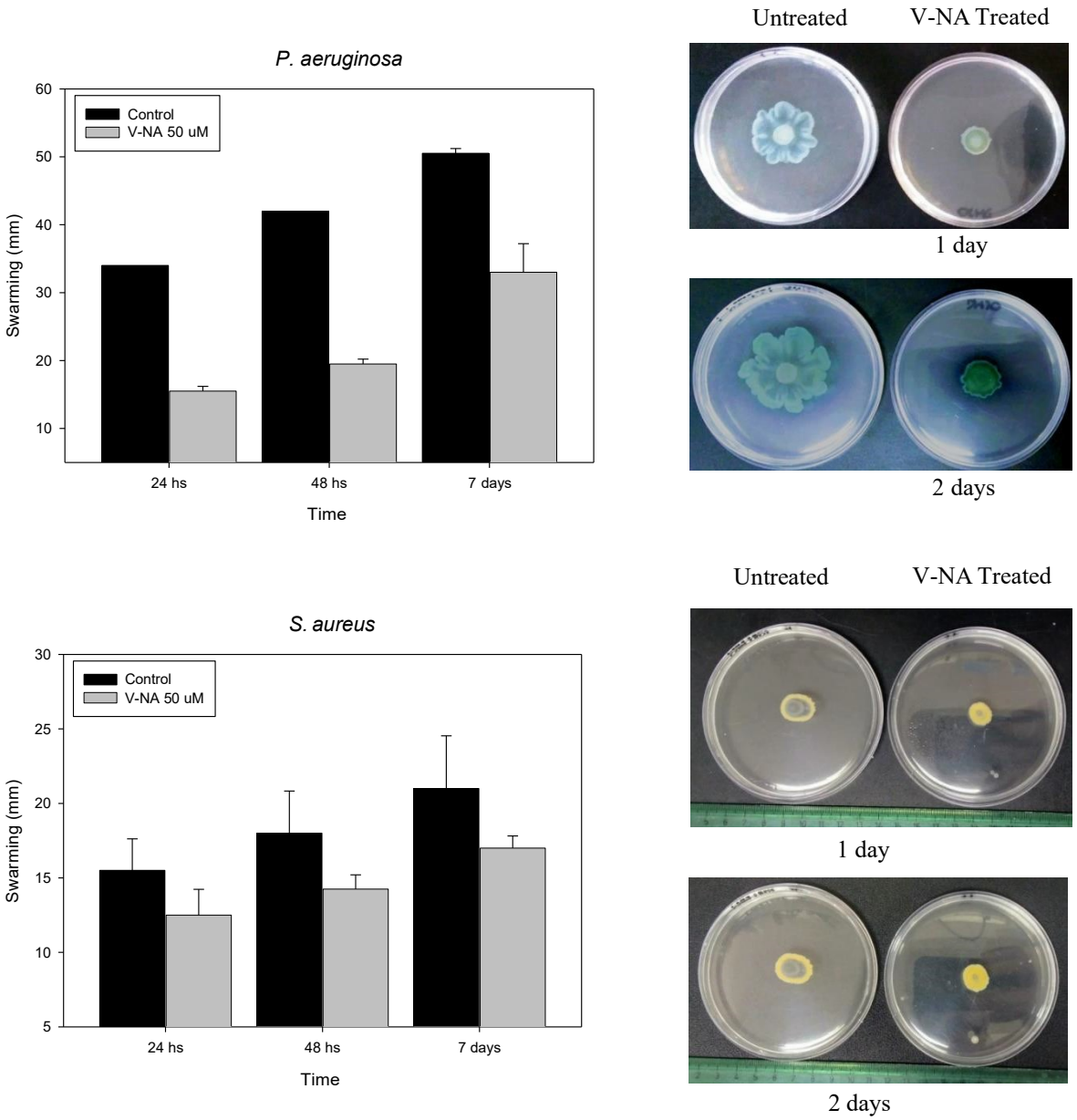

Figure 4.TEM micrographs of (a) empty and (b) V-NA loaded NLCs, and (c) empty and (d) V-NA loaded Eudragit nanoparticles.

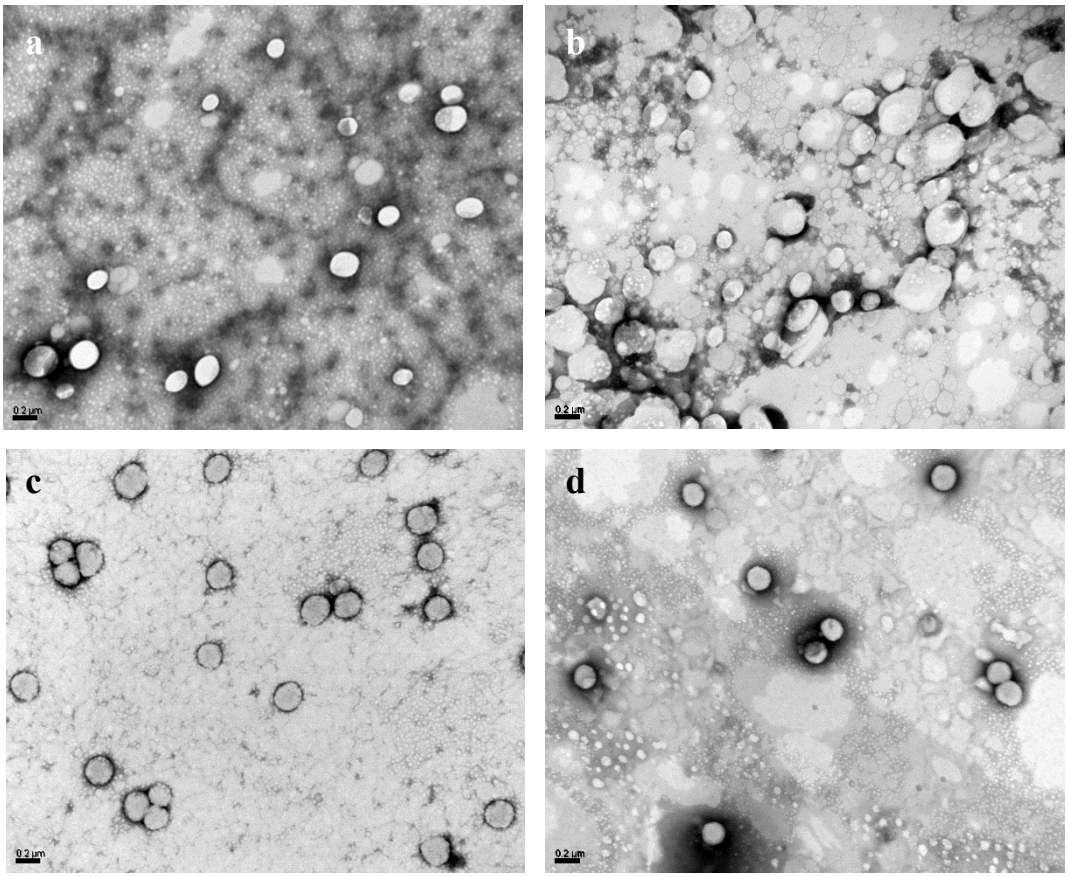

Figure 5. *In vitro* release profiles of V-NA from EuNPs and NLCs formulations.

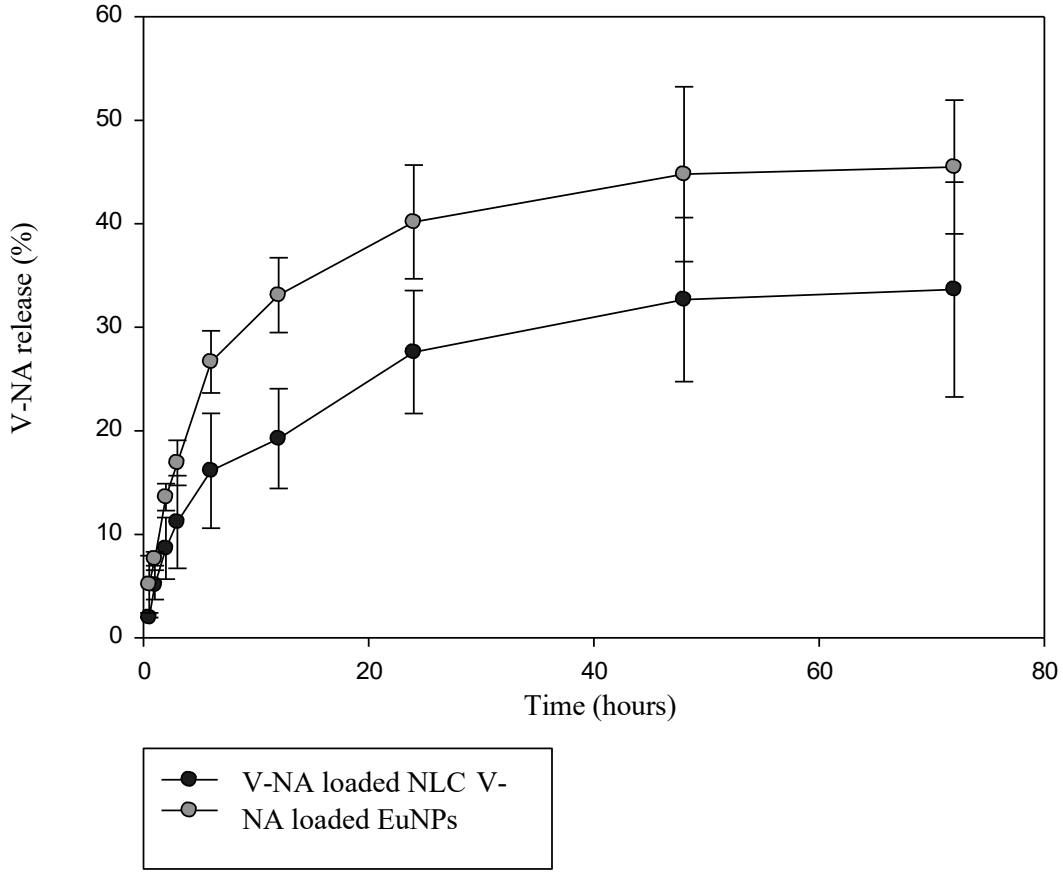

Figure 6. MIC values of V-NA loaded systems against *S. aureus* and *P. aeruginosa.*

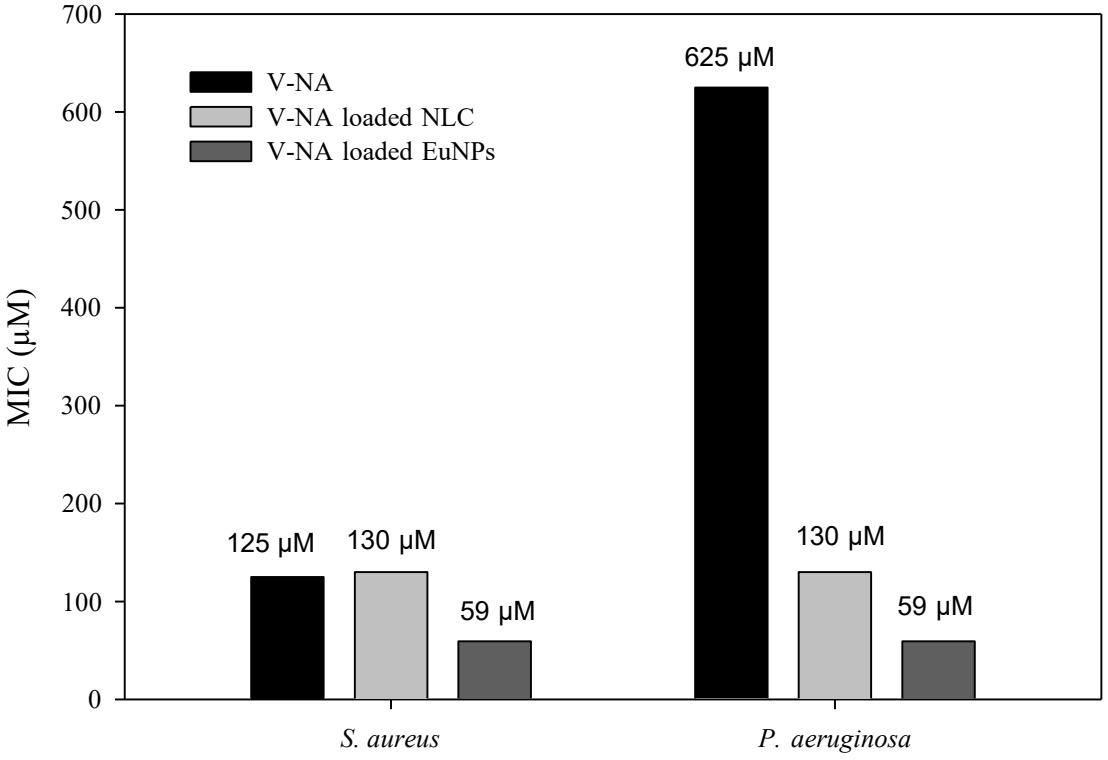

Figure 7. *Quorum sensing* inhibition assay in agar plates (I) and in microwell plates, after (II) and before (III) revealing with resazurin (dilutions 1/4 to 1/512). *C. violaceum* was used as reporter strain to assess QSI activity of V-NA (a), V-NA loaded NLCs (b) and V-NA loaded NLCs (c) at the indicated dilutions.

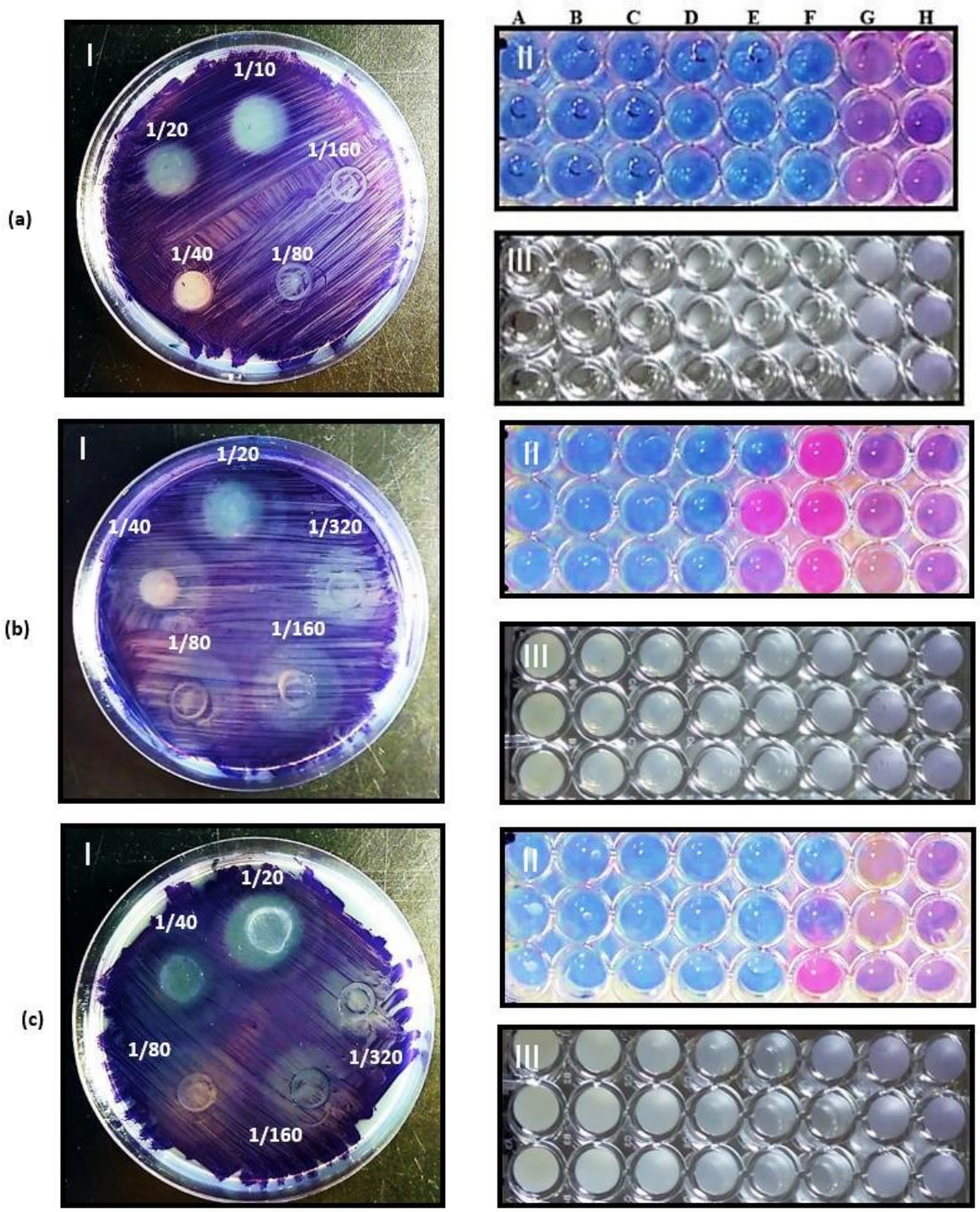

Figure 8. Dose-response analysis by MTT assay of cell viability of L929 cells when treated with NA and V-NA.

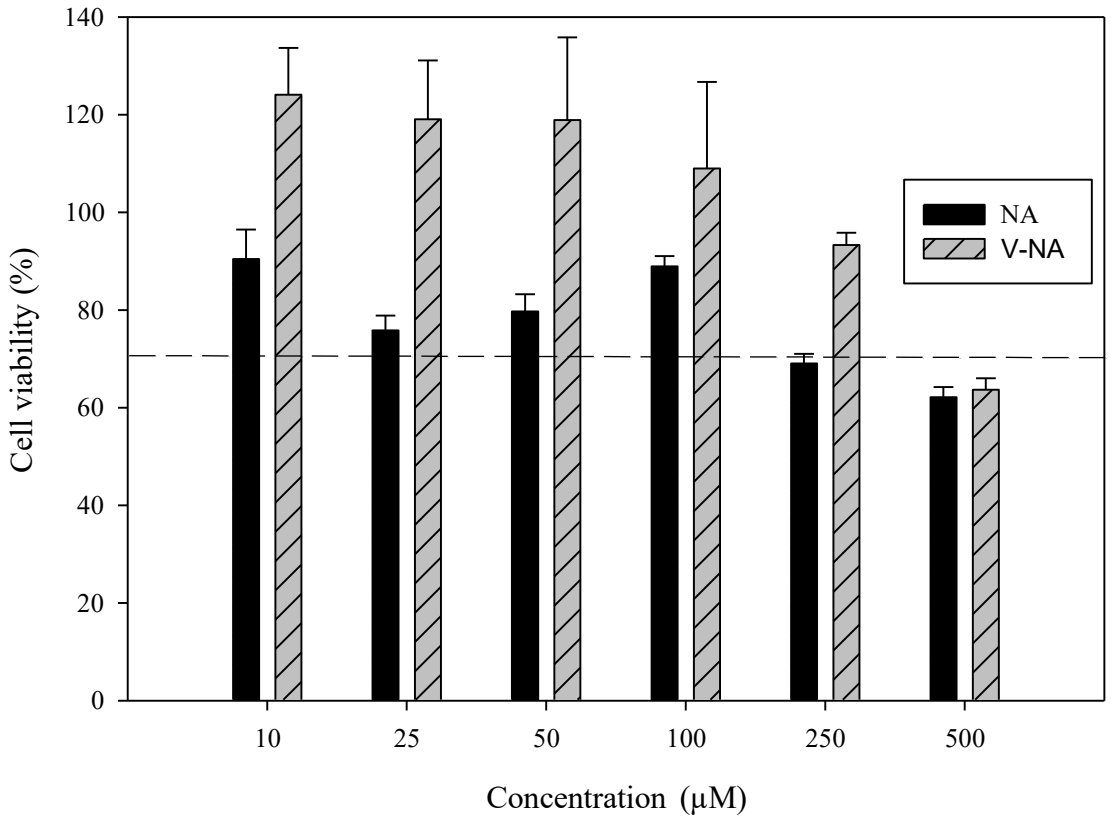

Figure 9. Dose-response analysis by MTT assay of cell viability of L929 cells treated with (a) V-NA loaded EuNPs and (b) V-NA loaded NLCs (relative to cell viability after treatment with the corresponding concentration of empty EuNPs and NLC, respectively). The horizontal dotted line indicates 70% threshold; above that, the formulation could be considered as non-cytotoxic under recommended levels set forth as guidelines by ISO and other standards organizations.

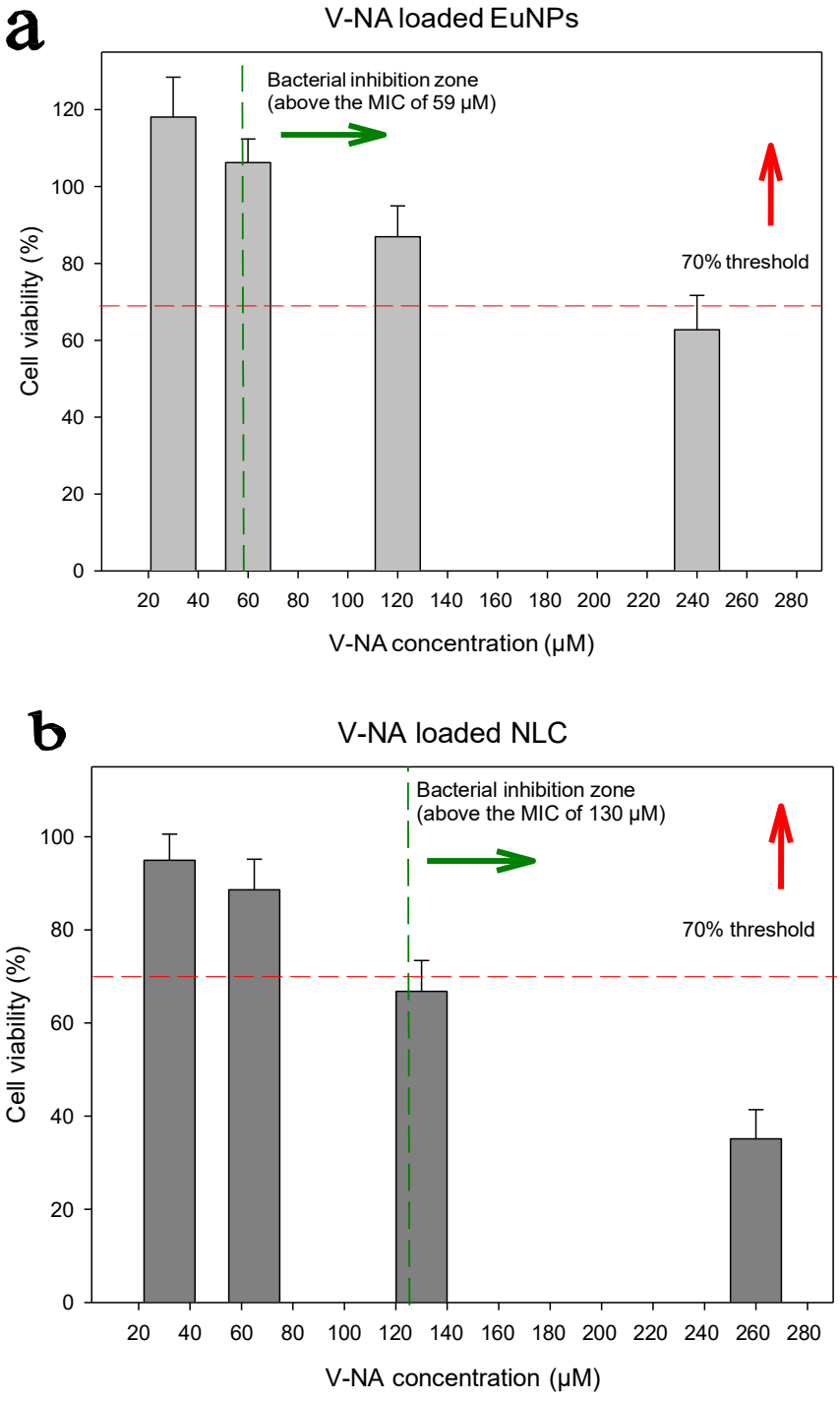

Tables

Table 1. *Minimum inhibitory concentration* (MIC) and *half maximal inhibitory concentration* (IC_{50}) for Nalidixic acid (NA) and the vanadium-NA complex (V-NA) tested in different ATCC strains.

	NA		V-NA		Reduction ratio (NA/V-NA)	
Strain	**MIC (µM)**	**IC_{50} (µM)**	**MIC (µM)**	**IC_{50} (µM)**	**MIC**	**IC_{50}**
E. coli	20.0	11.5	10.0	5.3	2.0	2.2
P. aeruginosa	1250.0	730.0	625.0	430.0	2.0	1.7
S. aureus	250.0	53.0	125.0	40.0	2.0	1.3
B. cereus	20.0	7.8	10.0	3.1	2.0	2.5

Table 2. Minimum bactericidal concentration (MBC) for V-NA free complex.

Strains	**MBC of V-NA complex (μM)**
Bacillus cereus	25.0-50.0
Escherichia coli	50.0
Pseudomonas aeruginosa	> 5,000.0
Staphylococcus aureus	250-500.0

Table 3. Particle size, polydispersity index (PDI) and Zeta potential (Z_{pot}) of empty and V-NA loaded formulations.

Samples		Mean size (nm)	PDI	Z_{pot} (mV)
NLC	Empty	236.9±2.2	0.211±0.009	13.98±1.05
	V-NA	331.6±5.1	0.278±0.011	11.22±1.08
EuNP	Empty	198.0±1.4	0.102±0,019	34.01±1.42
	V-NA	168.4±1.5	0.062±0.014	31.03±1.00